

El Niño Southern Oscillation (ENSO), Indian Ocean Dipole (IOD), and the Rise of Extreme Temperatures in Eastern Sumatra: Exploring Climate Change Dynamics

Hamdi Akhsan¹, Muhammad Irfan², Iskhaq Iskandar^{3*}

¹ Department of Physics Education Faculty of Teaching and Education, Sriwijaya University, Indonesia.

² Department of Physics Faculty of Mathematics and Natural Sciences, Sriwijaya University, Indonesia

³ Graduate School of Sciences, Faculty of Mathematics and Natural Sciences, Sriwijaya University, Indonesia.

Received: January 5, 2023

Revised: February 20, 2023

Accepted: February 25, 2023

Published: February 28, 2023

Corresponding Author:

Iskhaq Iskandar

iskhaq.iskandar@gmail.com

© 2023 The Authors. This open access article is distributed under a (CC-BY License)



DOI: [10.29303/jppipa.v9i2.3084](https://doi.org/10.29303/jppipa.v9i2.3084)

Abstract: The Indonesian region is affected by the monsoon system, which leads to a rainy season in December-March and a dry season in June-September. Global warming caused by human activities is increasing the risk of extreme climate events like floods, droughts, etc. The study aims to analyze the trends and correlations of extreme temperatures in the South Sumatra coastal area and its relationship with the DMI and Nino 3.4 indices. The four-stage research methodology includes data collection, extreme temperature index calculation, trend detection and correlation analysis with ENSO. Results indicate that the region has seen a rise in temperature, with hot day/night temperatures increasing by 0.26-0.29°C per decade and cold day/night temperatures by 2-3°C per 100-1000 years. A strong correlation was found between the DMI index and daily maximum/minimum temperatures, as well as between the Nino 3.4 index and the Diurnal Temperature Range (DTR). The study projects that nighttime temperatures will increase faster than daytime temperatures in the future, with a proportional correlation between the Nino 3.4 index and extreme temperatures.

Keywords: Climate Change; ENSO; ETCCDI; Extreme Temperatures; IOD.

Introduction

The Indonesian region experiences a climate that is significantly impacted by the monsoon system (Saha, 2010; Webster and Fasullo, 2003). The Asia-Australia monsoon, also known as the Southeast monsoon, prevails from June to September and blows from the Australian mainland towards the Asian mainland, whereas the Northwest monsoon, which operates from December to March, reverses the direction of the Southeast monsoon (Saha, 2010; Webster and Fasullo, 2003). Typically, the majority of Indonesia experiences a rainy season during the period of the Northwest monsoon (December-March) and a dry season during the period of the Southeast monsoon (June-September). The monsoon pattern can be disturbed at certain intervals by the equatorial Pacific region's El Niño-Southern Oscillation (ENSO) phenomenon (Philander,

1989) and the equatorial Indian Ocean region's Indian Ocean Dipole (IOD) ((Saji, Goswami, Vinayachandran, & Yamagata, 1999; Webster, Moore, Loschnigg, & Leben, 1999; Murtugudde, McCreary, & Busalacchi, 2000), leading to alterations in the rainfall patterns in Indonesia.

The Indonesian region is susceptible to fluctuations in rainfall levels based on the occurrence of the El Niño and positive IOD phenomenon, which result in a deficit in rainfall, while the La Niña and negative IOD lead to rainfall levels above the norm (Aldrian and Susanto, 2003; Hendon, 2003; Saji and Yamagata, 2003; Yamagata, Behera, Luo, Masson, Jury, & Rao, 2004; Juneng and Tangang, 2005; Iskandar, Lestari, Utari, Supardi, Rozirwan, Khakim, Poerwono, & Setiabudidaya, 2018; Lestari, Sutriyono, Sabaruddin, & Iskandar, 2018; Utari, Khakim, Setiabudidaya, & Iskandar, 2019). With the upward trend of global temperature, extreme climate

How to Cite:

Akhsan, H., Irfan, M. ., & Iskandar, I. . (2023). El Niño Southern Oscillation (ENSO), Indian Ocean Dipole (IOD), and the Rise of Extreme Temperatures in Eastern Sumatra: Exploring Climate Change Dynamics. *Jurnal Penelitian Pendidikan IPA*, 9(2), 600-608. <https://doi.org/10.29303/jppipa.v9i2.3084>

events are becoming increasingly prevalent, as highlighted in the Intergovernmental Panel on Climate Change (IPCC) special report on the impacts of global warming of 1.5°C above pre-industrial levels (IPCC, 2018). According to the IPCC reports, human activities, particularly the burning of fossil fuels, are the primary contributors to global warming (IPCC, 2013). Furthermore, human activities are also responsible for the increase in frequency of extreme rainfall and temperature events, as stated in previous IPCC reports (IPCC, 2012). The impact of rainfall and extreme temperature events in Asia has become a critical concern, leading to numerous studies being conducted, including works by (Choi, Kim, Kim, Kim, & Kim, 2009; Siswanto, van Oldenborgh, van der Schrier, Jilderda, & van den Hurk, 2016; Supari, Tangang, Juneng, & Aldrian, 2017; Supari, Tangang, Salimun, Aldrian, Sopaheluwakan, & Juneng, 2018; Supari, Tangang, Juneng, Cruz, Chung, Ngai, Salimun, Mohd, Santisirisomboon, Singhruck, PhanVan & Ngo-Duc, 2020; Lestari et al., 2018; Tan, Juneng, Tangang, Chung, & Firdaus, 2020).

A study conducted by Siswanto et al. (2016) in Jakarta, Indonesia utilized daily data collected over a period of 134 years and found that the frequency of extreme rainfall events (>50 mm/day) exhibited a positive trend from 1866-2010, with the highest increase occurring from 1966 to 2010. Additionally, the annual extreme temperatures in Jakarta increased by 1.6°C per century. The intensity and frequency of extreme rainfall events in Jakarta were observed to have a significant association with the El Niño Southern Oscillation (ENSO) and the Indian Ocean Dipole (IOD) phenomena, particularly during the dry season from June to November. However, this correlation weakened during the rainy season (Lestari et al., 2019). A study by Supari et al. (2017) revealed a warming trend in extreme indices in Indonesia from 1983-2012, with a continuous increase in annual extreme maximum and minimum temperatures of 0.18°/decade and 0.30°/decade respectively. Extreme rainfall displayed a trend towards wetter conditions, with a notable increase in daily rainfall intensity of 0.21 mm/day/decade. The trend towards wetter conditions was more prominent in the months of December-January-February (DJF) and March-April-May (MAM), however, a drying trend was observed in the months of June-July-August (JAS), September-October-November (SON), and MAM for regions in the southern equator.

The phenomenon of global warming has significantly elevated the likelihood of detrimental impacts of climate anomalies in Indonesia. These impacts may include the occurrence of floods, droughts, a decline in agricultural productivity, and the expansion of mosquito-borne diseases. This phenomenon has been recognized and discussed in several studies including

those by Hendon (2003), Marlier, Defries, Voulgarakis, Kinney, Randerson, Shindell, Chen, & Faluveg (2013), and Caminade, Kovats, Rocklov, Tompkins, Morse, Colón-González, Stenlund, Martens, & Lloyd (2014). In order to fully grasp the changes that have taken place in rainfall and temperature patterns in Indonesia, a number of research initiatives have been undertaken (Siswanto et al., 2016; Supari et al., 2017, 2018, 2020; Lestari et al., 2019).

However, research that specifically examines long-term extreme temperatures in the southern part of eastern Sumatra has not been conducted previously. Therefore, this study will comprehensively examine extreme temperatures and their relationship with the ENSO and IOD phenomena. The Extreme Temperature Index defined by the Expert Team on Climate Change Detection and Indices (ETCCDI) will be used in this study (Zhang, Alexander, Hegerl, Jones, Tank, Peterson, Trewin, & Zwiers, 2011). The present study employed daily rainfall data obtained from three different areas, including coastal, inland, and mountainous regions, for a period spanning from 1974 to 2016. The data was collected from 12 observation stations situated in the southern part of Eastern Sumatra and the time frame for this data was from 1981 to 2019. The purpose of this study is threefold: first, to examine the trend in extreme temperature in the southern part of Eastern Sumatra during the 1981-2019 period; second, to investigate the correlation between the Dipole Mode Index (DMI) and extreme temperature; and finally, to determine the relationship between the Niño 3.4 index and extreme temperature.

The anticipated outcomes of this research can be useful in the area of science, particularly in fields related to Indonesian climate parameters. By focusing on rainfall and temperature extremes in the southern coastal region of East Sumatra, this research has the potential to provide previously unknown insights that could transform our knowledge of this phenomenon. These findings can serve as the foundation for the establishment of mitigation strategies to prevent the negative effects of global warming, which is the responsibility of the government.

Method

The location of the present study encompasses the southern coastal region of Eastern Sumatra, comprising the provinces of Lampung, South Sumatra, Jambi, Riau, Riau Islands, and Bangka Belitung (as depicted in Figure 1). The data for rainfall, temperature, and air humidity were collected from the BMKG weather stations located in each of the aforementioned provinces, utilizing the rain gauges and temperature measuring instruments available at the BMKG stations. These instruments are

equipped with the capability to record the necessary meteorological data.



Figure 1. Location of the BMKG observation station for the Southern part of Sumatra

The location of the station where the study was conducted in its entirety is presented in Table 1.

Table 1. Research Location

| Location | Latitude | Longitude |
|-----------------|----------|-----------|
| Palembang | -2,927 | 104,772 |
| SMB II | -2,895 | 104,701 |
| Muaro Jambi | -1,602 | 103,484 |
| Sultan Taha | -1,634 | 103,640 |
| Japura Rengat | -0,330 | 102,320 |
| SSK II Pk. Baru | 0,45 | 101,44 |
| Panjang | -5,472 | 105,321 |
| R Intan | -5,160 | 105,110 |

Data and Procedures

The research will be conducted in four stages: 1) Data collection, quality control, and homogeneity analysis; 2) Calculation of general, hot, and cold ETCCDI extreme temperature indices, as listed in Table 2; 3) Trend detection and analysis using Mann-Kendall and Sens slope tests; and 4) Correlation analysis between the extreme temperature index and ENSO. To determine the characteristics of extreme temperatures in the South

Eastern coastal region of Sumatra, the data used in this research will be the maximum, minimum temperature data and temperature data recorded at 12 BMKG observation stations located in 6 provinces in the South Eastern coastal region of Sumatra during the period 1981-2019.

Quality Control (QC) and Homogeneity Test

Stooksbury, Idso, & Hubbard (1999) emphasized that missing or unrecorded temperature values in the data used can have a significant impact on trend analysis, therefore, quality control of the data is necessary to examine extreme temperatures. A Quality Control (QC) procedure is applied to detect and identify any errors that may occur in the process of recording, manipulating, formatting, transmitting, and archiving the data. To ensure accurate results of the analysis, this evaluation only uses data from observation stations that have at least 80% full years, where a full year is defined as a year where missing data does not exceed 15 days and there are no months with more than 3 days of missing data (Aguilar, Montagnani, Galvan, & Maisa, 2009; Supari et al., 2017, 2018). Observational data, especially if the observations are taken over a long period of time (>10 years), has a potential to contain shifts or spikes. These data shifts or spikes can occur naturally, such as ENSO and IOD climate anomalies. However, they can also be caused by technical (non-climatic) factors, such as changes in the environment around the observation point, relocation of measurement tools, changes in measurement procedures, as well as measurement tool errors or human error (Tank, Zwiers, & Zhang, 2009; Supari et al., 2017). In this study, homogeneity tests are performed using the RHtestsV4 software (<http://etccdi.pacificclimate.org/>). This application identifies potential changes that occur in the time series based on the F-test approach (Wang and Feng, 2013)

Extreme Temperature Index

In this study, only 11 temperature indices have been selected from the ETCCDI climate indices, as some indices, such as the freezing day index (FDO), growing season length (GSL), summer days (SU25), cold spell duration indicator (CSDI), and precipitation indices, are not applicable to the Indonesian region. The selected temperature indices comprise of those that measure the intensity and frequency of extreme events, as demonstrated in Table 2.

This study limited its analysis of the ETCCDI climate indices to only those that were relevant to the Indonesian region. As a result, only 11 temperature indices were selected that reflect the intensity and frequency of extreme events. These indices were then grouped into three categories for analysis. The first category, referred to as the general assessment group,

includes indices such as TXmean, TNmean, TMmean, and diurnal temperature range (DTR). The addition of TMmean was made to provide additional information on average temperature changes. The second group, focused on warm extreme indices, includes monthly maximum temperature maximum daily temperature (TXx), monthly maximum temperature minimum daily temperature (TNx), hot days (TX90p), and hot nights (TN90p). Finally, the third group, known as the cool group, consists of monthly minimum temperature maximum daily temperature (TXn), monthly minimum temperature minimum daily temperature (TNn), cool days (TX10p) and cool nights (TN10p). Descriptions of these extreme temperature indices can be found in Table 2. The calculation of the indices was done using the RCLimDex software and details of the calculations are described in Zhang and Yang (2004).

Table 2. Extreme Temperature Index

| Indicator Name | Definition of Indicator | Unit |
|---------------------------|---|------|
| Mean Tmax | Annual mean of maximum temperature | °C |
| Mean Tmin | Annual mean of minimum temperature | °C |
| Maximum Tmax | Monthly maximum value of daily max temperature | °C |
| Maximum Tmin | Monthly maximum value of daily min temperature | °C |
| Minimum Tmax | Monthly minimum value of daily max temperature | °C |
| Minimum Tmin | Monthly minimum value of daily min temperature | °C |
| Cool nights | Percentage of time when daily min temperature <10th percentile | % |
| Cool days | Percentage of time when daily max temperature < 10th percentile | % |
| Warm night | Percentage of time when daily min temperature > 90th percentile | % |
| Warm day | Percentage of time when daily max temperature > 90th percentile | % |
| Diurnal temperature range | Monthly mean difference between daily max and min temperature | °C |

Mann-Kendall & Sen's Slope

The non-parametric Mann-Kendall (MK) test was used in this study to assess trends in several climatic variables. In the discipline of hydroclimatology, the MK test is commonly used to find trends in time series data. The MK test's null hypothesis argues that there is no trend in the data, whereas the alternative hypothesis asserts that the data has a monotonic trend. If the Z value surpasses 1.96 at a 5% significance level, a significant trend is noticed, indicating the rejection of the null hypothesis. A positive Z number denotes an upward

trend, while a negative Z value indicates a downward trend (Hamed and Rao, 1998).

Correlation Analysis

Correlation analysis will be performed at this stage between extreme temperature indices and climate anomaly phenomena such as ENSO and IOD. The purpose of this correlation analysis is to determine how ENSO and/or IOD effect extreme temperatures along Sumatra's southern coast. The findings of this association analysis will also be compared to data on land fires in southern Sumatra, particularly during El Niño and positive IOD years such as 1982/1983, 1997/1998, 2006, 2015/2016, and 2019.

Result and Discussion

Data Quality Control

Daily data from 20 BMKG stations in four provinces range in time from 40 years (1981-2020) to four years (2017-2020). The first phase is to choose stations with more than 20 years of data; from this step, 14 (fourteen) stations are obtained. The next stage is to do manual Quality Control (QC) (using the Microsoft Excel 2019 program) to discover and identify problems that may arise during the recording, manipulation, formatting, transferring, and archiving of data. This study only includes data from observation stations that have at least 80% of the year covered, with a full year defined as a year with no more than 15 days of missing data and no months. Following the manual QC procedure, 8 BMKG stations in Southern Sumatra met the standards to proceed to the second phase of the QC procedure. The second stage of the technique employs RCLimdex Extra QC software, which detects outliers by exceeding the interquartile range (IQR). Based on observations from all years, the IQR, upper and lower bounds were determined for each month. If a value is outside the range of the lower and upper boundaries, it is suspected of being an outlier. to provide the initial Image output per station for the selected 8 (eight) stations.

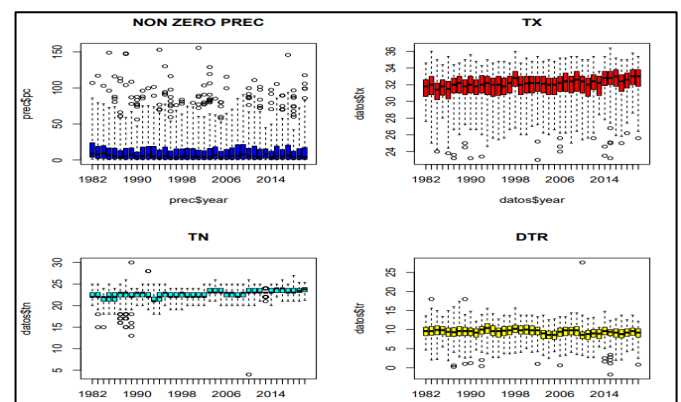


Figure 2. Results of QC analysis for TN, TX, and in SM Japura Rengat 1981-2020

The following is a summary of the RCLimindex additional QC results for one of the BMKG stations used, which were manually entered into the computer and checked. The display that emerges will then look like in Figure 2. The same technique is followed for the remaining 7 stations so that the data justified at this stage can be incorporated in the following process, namely the Homogenization test.

Homogenization test

The RHtestsV4 software was used to perform homogeneity tests in this research. Based on the F-test technique, this program finds probable changes in a time series. The data homogeneity test is performed to re-check aberrant data that was not found or overlooked in the preceding procedure, as well as for data homogenization. The data was homogenized using statistical methodologies agreed upon by climatologists. Only data for Tx and Tn can be evaluated for homogeneity using RH testv4 (it cannot be done for RR rainfall). The first output of the RHtestsV4 homogeneity test is the original image of daily Tmax and Tmin, which will be homogenized as demonstrated in the following example results:

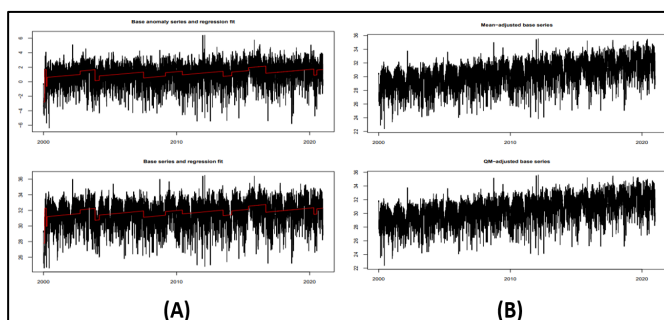


Figure 3. The results of the RH Test for SK Muaro Jambi Maximum Temperature data daily

The results of the homogeneity test, which did not use a reference series, could have implications for detecting natural climate processes such as inhomogeneity due to El Niño effect non specific years. All other stations whose data were used in this investigation had the RH test performed. The data is then utilized to compute the extreme climate index using the technique proposed by the Climate Change Detection and Index Expert Team after the QC and homogenization processes (ETCCDI).

Non-parametric Mann-Kendall (MK) test trend estimation

Trends are evaluated at the 95% confidence level. Trends are evaluated using the MK test. The indices of each station are averaged to provide a single time series of indices that may be used to estimate regional-level trends. Table 3 demonstrates that on average, 48% of the trend of the index data is significant at the 99% level, 14% is significant at the 97.5% level, 14% is significant at the

95% level, 2% is positive but not significant, and 21% is not significant. This suggests that 76% of the trend index data assessed with non-parametric Mann-Kendall is significant at the 95% level, whereas 21% is not. The percentage index significance diagram in Figure 3 provides an overview of the relevance of the Mann-Kendall trend for each index data.

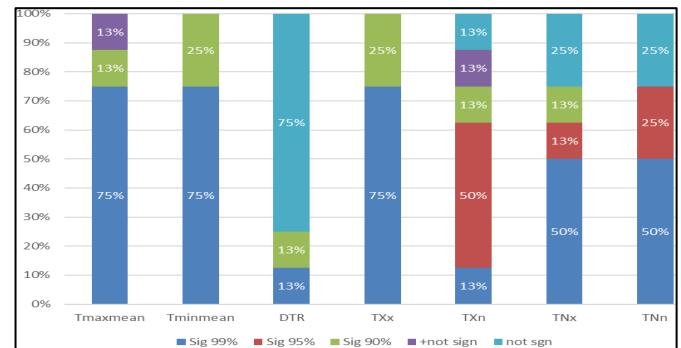


Figure 4. Percentage Significance of the index by Trend MK Test

Extreme temperature trends

The Extreme Warm Index (EWI) will climb with strong geographic consistency. 75% of stations show a 95% confidence increase in the warmest daytime temperature (TXx). 25% of stations are significant. All stations show a warming trend in the coldest temperature of the day (TXn), with 76% of the trends being statistically significant. Table 4 shows that TXx and TNx region-level trends have increased 0.26°C and 0.29°C each decade, respectively. These data demonstrate the rising trend and its effects on local climate. Figure 4 shows that without significant effort, the average maximum and minimum temperatures (TMINMean) will rise 2.6°C every millennium. Over a millennium, DTR dropped 3.1°C because the max daily temperature warmed slower than the min. High spatial coherence and trend augmentation improve the warm extreme index, including the hottest day (TXx) and night (TNx). The hottest day (TXx) climbs 2.61% each 100 years, and the warmest night (TNx) rises 3°C per 100 years.

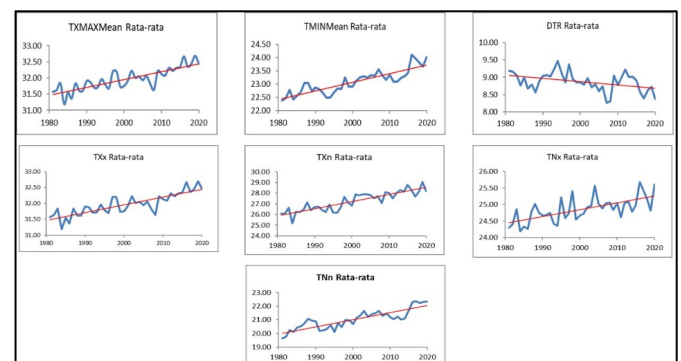


Figure 5. Trend Estimated increase in temperature extreme index over 4 decades (increase per 10 years)

The findings of the study point to a discernible upward trend in the extreme cold index, which takes into account both the coldest daily temperatures (TXn) and the lowest overnight temperatures (TNn). The temperature of the coldest day and night has exhibited a significant increase at the regional level of Southern Sumatra, with a pace of 0.2°C every decade, which is equivalent to 2°C per century and 3°C per millennium, respectively. The findings of the investigation into the extreme temperature index will be correlated with the El Nio-Southern Oscillation (ENSO), as well as the Indian Ocean Dipole (IOD). The NINO 3.4 index will be used to represent ENSO data, and the DMI index will be used to represent IOD data. Both indices will be utilized in the analysis.

DMI Correlation with Extreme Temperature

The correlation between the extreme temperature index and the EIOD was investigated using DMI data

from 1981 to 2020, a period of 40 years and 12 months in a single year. For the next 40 years, the best value for the DMI is between August-September-October-November (ASON). The Pearson correlation statistic was utilized to connect the results of the two averages, with variable X representing the DMI index and variable Y representing the extreme temperature index, and the overall average value was calculated in table 5.

The Pearson correlation index table (Table 6) between the DMI index and the index of each temperature from each station shows that the DMI index has a 99% significant correlation with the average maximum temperature (TMAXmean) with a value of $r = 0.454$. This association is the same as the 0.551 correlation coefficient between the DMI index and the warmest temperature of the day (TXx). These two facts demonstrate that the DMI index, which rises year after year, has a direct and strong correlation with TMAXMean and TXx.

Table 3. Index trend of non-parametric MK test data per station

| Station | TMAX Mean | TMIN mean | DTR | TXx | TXn | TNx | TNn |
|----------------|-----------|-----------|--------|-------|-------|--------|-------|
| Palembang | 0.047 | 0.043 | 0.005 | 0.050 | 0.048 | 0.000 | 0.056 |
| SMB II | 0.036 | 0.034 | 0.011 | 0.050 | 0.047 | 0.000 | 0.000 |
| Muaro Jambi | 0.041 | 0.041 | 0.004 | 0.038 | 0.060 | 0.050 | 0.050 |
| Sultan Taha | 0.020 | 0.020 | -0.010 | 0.020 | 0.019 | 0.020 | 0.020 |
| Japura Rengat | 0.041 | 0.039 | -0.013 | 0.035 | 0.025 | 0.027 | 0.021 |
| SSK II Pk.Baru | 0.012 | 0.013 | -0.041 | 0.033 | 0.024 | 0.057 | 0.067 |
| Panjang | 0.037 | 0.037 | 0.014 | 0.033 | 0.033 | -0.020 | 0.050 |
| R Intan | 0.033 | 0.033 | -0.002 | 0.029 | 0.036 | 0.031 | 0.033 |
| Overall trend | 0.266 | 0.261 | -0.031 | 0.288 | 0.292 | 0.165 | 0.297 |

Table 4. Index Trend Estimation based on individual station in Southern Sumatra region

| Index | Overall Trend (°C) | Station Trend (°C) |
|----------|--------------------|--------------------|
| TMAXmean | 0.266 | 0.012 s.d 0.043 |
| TMINmean | 0.261 | 0.013 s.d 0.043 |
| DTR | -0.031 | -0.041 s.d 0.005 |
| TXx | 0.261 | 0.020 s.d 0.050 |
| TXn | 0.292 | 0.019 s.d 0.060 |
| TNx | 0.202 | 0.000 s.d 0.057 |
| TNn | 0.297 | 0.000 s.d 0.067 |

Table 5. Pearson correlation index between the DMI index and the temperature index

| Station | SK Palembang | SM SMB II | SK M. Jambi | SM S. Taha | SK Japura | SM SSK | SMM Panjang | SM R Intan | R Index Average |
|-----------------|--------------|-----------|-------------|------------|-----------|--------|-------------|------------|-----------------|
| Df = N-1 | 36 | 36 | 19 | 34 | 37 | 33 | 21 | 38 | |
| TMAXmean vs DMI | 0.532 | 0.562 | 0.308 | 0.148 | 0.245 | -0.144 | 0.252 | 0.604 | 0.454 |
| TMINmean vs DMI | 0.186 | -0.046 | 0.177 | 0.257 | 0.292 | 0.130 | 0.071 | 0.164 | 0.252 |
| R DTR vs DMI | 0.553 | 0.443 | 0.235 | -0.088 | -0.092 | -0.205 | -0.058 | 0.402 | 0.159 |
| R TXx vs DMI | 0.517 | 0.637 | 0.143 | 0.139 | 0.168 | 0.117 | 0.196 | 0.459 | 0.551 |
| R TXn vs DMI | 0.221 | 0.292 | 0.116 | -0.077 | 0.212 | 0.145 | 0.183 | 0.355 | 0.355 |
| R TNx vs DMI | 0.066 | -0.079 | 0.109 | 0.291 | 0.071 | 0.034 | 0.114 | 0.246 | 0.065 |
| R TNn vs DMI | 0.204 | -0.157 | 0.247 | 0.119 | 0.216 | 0.145 | 0.117 | 0.059 | 0.296 |

Table 6. Significance of Pearson's correlation index between DMI and temperature index

| Index | SK Palembang | SM SMB II | SK M. Jambi | SM S. Taha | SK Japura | SM SSK | SMM Panjang | SM R Intan | R Index Average |
|-----------------|--------------|-----------|-------------|------------|-----------|--------|-------------|------------|-----------------|
| TMAXmean vs DMI | **** | **** | * | + | * | - | + | **** | **** |
| TMINmean vs DMI | + | - | + | - | ** | + | + | + | * |
| R DTR vs DMI | **** | **** | + | - | - | - | + | **** | *** |
| R TXx vs DMI | **** | **** | + | * | + | + | + | **** | **** |
| R TXn vs DMI | * | ** | + | - | * | + | + | *** | *** |
| R TNx vs DMI | + | - | + | ** | + | + | + | * | + |
| R TNn vs DMI | + | - | * | + | * | + | + | + | ** |

The tendency of each gradient clearly illustrates the correlational relationship between the DMI Index and the average maximum temperature and the hottest temperature during the day, which clearly indicates a correlational increasing trend between the three. The TMaxmean and TXx indices are improving. The increase/increase in the average maximum daytime temperature is faster than the increase/increase in the average hottest daytime temperatures every decade (Figure 6).

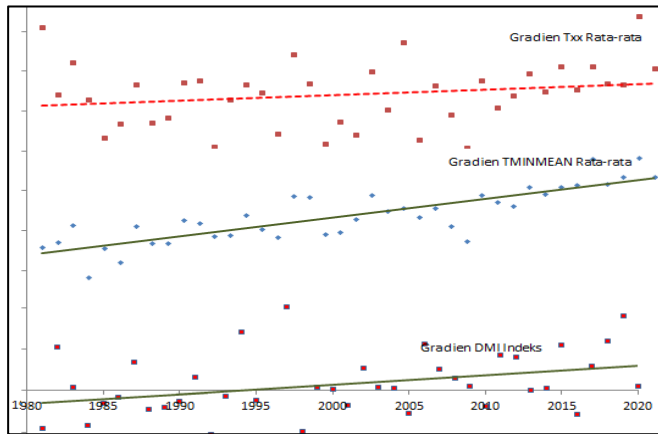


Figure 6. Comparison of Trends in DMI, TMAXMean, and TXx for All Southern Sumatra Stations

Nino 3.4 Correlation with Extreme Temperatures

The correlation between the extreme temperature index and the Nino 3.4 index was analyzed by utilizing data collected over a 40-year period, from 1981 to 2020,

with a monthly interval of 12 months in a year. The best values for the Nino 3.4 index were recorded during the months of September, October, November, and December, as well as June to December.

To calculate the Pearson correlation coefficient, data from each station was evaluated, and the results were presented in Table 7. The Pearson correlation coefficient between the Nino 3.4 index and the extreme temperature index was calculated and presented in Table 8. Significance levels of 99%, 97.5%, 95%, and 90% were used to interpret the results from the Pearson correlation coefficient table.

The Pearson DMI correlation results at severe temperatures revealed a different outcome than the results obtained at other temperatures. When the DTR (diurnal temperature range) was taken into account, the association between the Nino 3.4 index and the extreme temperature index was determined to be extremely significant at a 97.5% confidence level. The association between the average maximum temperature (TMaxmean) and the highest temperature during the day (Txx), on the other hand, was shown to be significant at a 90% significance level. The Pearson correlation coefficient computed between the Nino 3.4 index and the extreme temperature index was 0.852. Nino 3.4 immediately raises both severe heat indices. Nino negatively affects the average lowest, hottest, and coldest overnight temperatures, however this correlation is not statistically significant. The day's coldest temperature is positively correlated with Nino, although not statistically significant.

Table 7. Pearson correlation index between Nino 3.4 and extreme temperature index

| Index | SK Palembang | SM SMB II | SK M. Jambi | SM S. Taha | SK Japura | SM SSK | SMM Panjang | SM R Intan | R Index Average |
|------------|--------------|-----------|-------------|------------|-----------|--------|-------------|------------|-----------------|
| df = N-2 | 36 | 36 | 19 | 34 | 37 | 33 | 21 | 38 | |
| RTMAXMea n | 0.279 | 0.329 | 0.349 | 0.108 | 0.015 | -0.119 | 0.268 | 0.380 | 0.201 |
| RTMINMea n | -0.215 | -0.276 | -0.131 | -0.089 | -0.074 | -0.066 | 0.099 | -0.117 | -0.109 |
| R DTR | 0.581 | 0.463 | 0.559 | 0.155 | 0.114 | -0.017 | -0.045 | 0.471 | 0.285 |
| R TXx | 0.268 | 0.268 | 0.221 | 0.061 | 0.053 | 0.101 | 0.241 | 0.567 | 0.223 |
| R TXn | -0.018 | -0.050 | 0.099 | 0.036 | 0.124 | 0.018 | 0.282 | 0.190 | 0.085 |
| R TNx | -0.278 | -0.215 | -0.171 | -0.066 | -0.087 | -0.028 | 0.200 | 0.016 | -0.079 |
| R TNn | -0.155 | -0.265 | -0.090 | -0.103 | -0.016 | -0.083 | 0.066 | -0.175 | -0.103 |

Table 8. Correlation of the Nino 3.4 index with extreme temperatures

| Index | SK Palembang | SM SMB II | SK M. Jambi | SM S.Taha | SK Japura | SM SSK | SMM Panjang | SM R Intan | Average |
|-----------|--------------|-----------|-------------|-----------|-----------|--------|-------------|------------|---------|
| RTMAXMean | ** | *** | * | + | + | - | * | **** | * |
| RTMINMean | * | *** | - | - | - | - | + | - | - |
| R DTR | **** | **** | **** | + | - | - | - | **** | ** |
| R TXx | ** | * | * | + | + | - | + | **** | * |
| R TXn | - | - | + | - | + | + | + | + | + |
| R TNx | ** | * | - | - | - | - | + | + | - |
| R TNn | - | ** | - | - | - | - | + | - | - |

Conclusion

The South Sumatra coastal region has experienced a rise in temperature with an increase of 0.26°C to 0.29°C per decade in hottest day temperature and average night temperature. The trend of warming can be seen in the coldest day and night temperatures, which have increased significantly by 2°C per hundred years and 3°C per millennium, respectively. The correlation between the DMI index and average maximum temperature (TMaxmean) was found to be highly significant, with a significance level of 99% and a correlation coefficient of 0.454. A significant positive relationship was also found between the DMI index and minimum daily temperature during the day and night, indicating that an increase in the DMI index is directly related to the increase in temperature. The correlation between the Nino 3.4 index and extreme temperature indices was only significant for the Diurnal Temperature Range (DTR) with a Pearson correlation coefficient of 0.852. The nighttime temperature is expected to increase faster in the coming decade compared to the average daytime temperature and the correlation between the Nino 3.4 index and extreme temperature indices will be significantly proportional.

References

Aguilar, E., Montagnani, L., Galvan, D., & Maisa, A. (2009). Changes In Temperature And Precipitation Extremes In Western Central Africa, Guinea Conakry, And Zimbabwe, 1955-2006. *Journal of Geophysical Research: Atmospheres*, 114(2). <https://doi.org/10.1029/2008JD011010>.

Aldrian, E., Karmini, M., & Budiman. (2011). *Adaptasi Dan Mitigasi Perubahan Iklim Di Indonesia*. Jakarta, Indonesia: Pusat Perubahan Iklim dan Kualitas Udara BMKG.

Badan Nasional Penanggulangan Bencana. (2016). *Ancaman Hidrometeorologi Semakin Meningkat*. Jakarta, Indonesia: Gema BNPB.

Caminade, C., Kovats, S., Rocklov, J., Tompkins, A. M., Morse, A. P., Colón-González, F. J., Stenlund, H., Martens, P., & Lloyd, S. J. (2014). Impact Of Climate Change On Global Malaria Distribution. *Proceedings Of The National Academy Of Sciences Of The United States Of America*, 111(9), 3286-3291.

<https://doi.org/10.1073/pnas.1302089111>.

Choi, G., Kim, Y. J., Kim, S. W., Kim, S. H., & Kim, J. H. (2009). Changes In Means And Extreme Events Of Temperature And Precipitation In The Asia-Pacific Network Region, 1955-2007. *International Journal of Climatology*, 29, 1906-1925. <https://doi.org/10.1002/joc.1979>

Hendon, H. H. (2003). Indonesian Rainfall Variability: Impacts of ENSO and Local Air-Sea Interaction. *Journal of Climate*, 16, 1775-1790. <https://doi.org/10.1175/1520-0442>

IPCC. (2012). *Managing The Risks Of Extreme Events And Disasters To Advance Climate Change Adaptation*. A Special Report Of Working Groups I And II Of The Intergovernmental Panel On Climate Change. Cambridge, United Kingdom And New York, NY: Cambridge University Press. Retrieved from <https://www.ipcc.ch/report/managing-the-risks-of-extreme-events-and-disasters-to-advance-climate-change-adaptation/>

IPCC. (2013). *Climate Change 2013: The Physical Science Basis. Contribution Of Working Group I To The Fifth Assessment Report Of The Intergovernmental Panel On Climate Change*. Cambridge, United Kingdom And New York, NY: Cambridge University Press. <https://doi.org/10.1017/CBO9781107415324>

IPCC. (2018). *IPCC Special Report On The Impacts Of Global Warming Of 1.5°C*. Retrieved from: <https://www.ipcc.ch/sr15/>

Iskandar, I., Lestari, D. O., Utari, P. A., Supardi, Rozirwan, Khakim, M. Y. N., Poerwono, P., & Setiabudidaya, D. (2018). Evolution and impact of the 2016 negative Indian Ocean Dipole. *Journal of Physics: Conference Series*, 985(1). <https://doi.org/10.1088/1742-6596/985/1/012017>.

Lestari, D. O., Sutriyono, E., Sabaruddin, S., & Iskandar, I. (2018). Respective influences of Indian Ocean Dipole and El Niño-Southern Oscillation on Indonesian precipitation. *Journal of Mathematical Fundamental Sciences*, 50(3), 257-272. <https://doi.org/10.5614/j.math.fund>

Marlier, M. E., Defries, R. S., Voulgarakis, A., Kinney, P. L., Randerson, J. T., Shindell, D. T., Chen, Y., & Faluvegi, G. (2013). El Niño and health risks from landscape fire emissions in southeast Asia. *Nature Climate Change*, 3(2), 131-136.

- <https://doi.org/10.1038/nclimate1658>
- Philander, S. G. (1989). *El Niño, La Niña, and the Southern Oscillation*. Academic Press, 46, 293.
- Saha, K. (2010). *Tropical Circulation Systems and Monsoons*. Springer-Verlag Berlin Heidelberg, New York.
- Saji, N. H., & Yamagata, T. (2003). Structure Of SST And Surface Wind Variability During Indian Ocean Dipole Mode Events: COADS Observations. *Journal of Climate*, 16(16), 2735-2751. <https://doi.org/https://doi.org/10.1175/1520-0442>
- Saji, N. H., Goswami, B. N., Vinayachandran, P. N., & Yamagata, T. (1999). A Dipole Mode In The Tropical Indian Ocean. *Nature*, 401(6751), 360-363. <https://doi.org/10.1038/43854>
- Siswanto, S., van Oldenborgh, G. J., van der Schrier, G., Jilderda, R., & van den Hurk, B. (2016). Temperature, Extreme Precipitation, And Diurnal Rainfall Changes In The Urbanized Jakarta City During The Past 130 Years. *International Journal of Climatology*, 36(9), 3207-3225. <https://doi.org/10.1002/joc.4548>
- Stooksbury, D. E., Idso, C. D., & Hubbard, K. G. (1999). The Effects Of Data Gaps On The Calculated Monthly Mean Maximum And Minimum Temperatures In The Continental United States: A Spatial And Temporal Study. *Journal of Climate*, 12, 1524-1533. <https://doi.org/10.1175/1520-0442>
- Supari, Tangang, F., Juneng, L., Cruz, F., Chung, J. X., Ngai, S. T., Salimun, E., Mohd, M. S., Santisirisomboon, J., Singhruck, P., PhanVan, T., Ngo-Duc, T., Narisma, G., Aldrian, E., Gunawan, D., & Sopaheluwakan, A. (2020). Multi-model projections of precipitation extremes in Southeast Asia based on CORDEX-Southeast Asia Simulations. *Environmental Research*, 184, 109350. <https://doi.org/10.1016/j.envres.2020.109350>
- Supari, F., Tangang, F., Juneng, L., & Aldrian, E. (2017). Observed Changes In Extreme Temperature And Precipitation Over Indonesia. *International Journal Of Climatology*, 37(4), 1979-1997. <https://doi.org/10.1002/joc.4829>
- Supari, F., Tangang, F., Salimun, E., Aldrian, E., Sopaheluwakan, A., & Juneng, L. (2018). ENSO Modulation Of Seasonal Rainfall And Extremes In Indonesia. *Climate Dynamics*, 51(7), 2559-2580. <https://doi.org/10.1007/s00382-017-4028-8>
- Tan, M. L., Juneng, L., Tangang, F. T., Chung, J. X., & Firdaus, R. B. R. (2020). Changes In Temperature Extremes And Their Relationship With ENSO In Malaysia From 1985 To 2018. *International Journal of Climatology*, 41(S1). <https://doi.org/10.1002/joc.6864>
- Tank, K. A. M., Zwiers, F. W., & Zhang, X. (2009). *Guidelines On Analysis Of Extremes In A Changing Climate In Support Of Informed Decisions For Adaptation*. Geneva, Switzerland. Retrieved from: https://www.ecad.eu/documents/WCDMP_72_TD_1500_en_1.pdf
- Utari, P. A., Khakim, M. Y. N., Setiabudidaya, D., & Iskandar, I. Dipole, (2019). Dynamics of 2015 positive Indian Ocean. *Journal of Southern Hemisphere Earth System Science*, 69(1), 75. <https://doi.org/10.1071/es19002>
- Wang, X. L., & Feng, Y. (2013). *RHtestsV4 User manual*. Climatic Research Division, Atmospheric Science and Technology Directorate, Science and Technology Branch, Environment Canada. Retrieved from: http://etccli.pacificclimate.org/RHtest/RHtestsV4_UserManual_10Dec2014.pdf
- Webster, P. J., Moore, A., Loschnigg, J. P., & Leben, R. R. (1999). Coupled Ocean-Atmosphere Dynamics In The Indian Ocean During 1997-98. *Nature*, 401(6751), 356-360. <https://doi.org/10.1038/43848>
- Webster, P.J. and Fasullo, J., 2003. Encyclopedia of Atmospheric Sciences. *Holton, J. & Curry, JA (eds.)*, pp.1370-1386. <https://doi.org/10.1016/B0-12-227090-8/00236-0>
- Worldometer. (2022). *CO2 emissions by country*. Worldometer - real time world statistics. Retrieved from: <https://www.worldometers.info/co2-emissions/co2-emissions-by-country/>
- Yamagata, T., Behera, S. K., Luo, J., Masson, S., Jury, M. R., & Rao, S. A. (2004). Coupled Ocean-Atmosphere Variability In The Tropical Indian Ocean. *Geophysical Monograph Series*, 147, 189-211. <https://doi.org/10.1029/147GM12>
- Zhang, X., Alexander, L., Hegerl, G. C., Jones, P., Tank, A. K., Peterson, T. C., Trewin, B., & Zwiers, F. W. (2011). Indices For Monitoring Changes In Extremes Based On Daily Temperature And Precipitation Data. *Wiley Interdisciplinary Reviews: Climate Change*, 2(6), 851-870. <https://doi.org/10.1002/wcc.147>